Thermochimica Acta, 215 (1993) 143–155
Elsevier Science Publishers B.V., Amsterdam

The influence of ferric oxide on the properties of $3CaO \cdot 3Al_2O_3 \cdot SrSO_4$ [1]

Dun Chen [a], Xiuji Feng [b] and Shizhong Long [b]

[a] *Dept. of Chemistry, The University of Toledo, OH 43606 (USA)*
[b] *Dept. of Materials Sciences, The Wuhan University of Technology, Hubei 430070 (People's Republic of China)*

(Received 11 May 1992)

Abstract

It was determined that at 18.84 wt.% Fe_2O_3 reached a maximum solid solution in $3CaO \cdot 3Al_2O_3 \cdot SrSO_4$ by replacing Al_2O_3. The physical properties of the compound with and without Fe_2O_3 were measured and these are combined with the analysis of the hydration process and products by using XRD, DTA and calorimetric equipment to determine the heat of hydration, etc. The results show that there was no tricalcium aluminate hexahydrate ($3CaO \cdot Al_2O_3 \cdot 6H_2O$) formed in any of the samples. The addition of Fe_2O_3 to $3CaO \cdot 3Al_2O_3 \cdot SrSO_4$ caused a decrease in the compressive strength. Among the hydration products, two hydrates in the form of $3CaO \cdot Al_2O_3 \cdot 3SrSO_4 \cdot nH_2O$ and $3CaO \cdot Al_2O_3 \cdot SrSO_4 \cdot nH_2O$ were found.

INTRODUCTION

After the important compound, $3CaO \cdot 3Al_2O_3 \cdot CaSO_4$ was identified in cements in the 1960s, compounds of the form $3CaO \cdot Al_2O_3 \cdot M_x(SO_4)_y$ ($M = Mg^{2+}$, Sr^{2+}, Ba^{2+}, Fe^{3+}, Al^{3+}) were studied [1] by Teoreanu et al. They claimed to have found a series of compounds by heating mixtures of $M_x(SO_4)_y$ with $CaCO_3$ and Al_2O_3 at 1400°C for 4 h. From the most recent research [2] on the derivatives of $3CaO \cdot 3Al_2O_3 \cdot CaSO_4$ by substituting the $CaSO_4$ by $SrSO_4$ or $BaSO_4$, it has been shown that Teoreanu et al. did not produce these compounds. Only at appropriate temperatures can these compounds be prepared.

The cementation properties of $3CaO \cdot 3Al_2O_3 \cdot SrSO_4$ have, however, been reported [2]. To further this kind of investigation and make it possible to produce a new kind of cement, in the present study Fe_2O_3 was added to $3CaO \cdot 3Al_2O_3 \cdot SrSO_4$ in the hope that it might decrease the

Correspondence to: D. Chen, Dept. of Chemistry, The University of Toledo, OH 43606, USA.

[1] Cement chemists' notation: C = CaO; A = Al_2O_3; F = Fe_2O_3; H = H_2O.

manufacturing temperature and increase the ability to withstand grinding. The properties of this series of compounds, which is called the SF system, are reported in this study. The maximum percentage of the replacement of aluminium oxide by ferric oxide is studied. Further, by following the hydration process, more information is obtained.

EXPERIMENTAL

Material

Various ratios of analytical reagents, calcium carbonate ($CaCO_3$), aluminum oxide (Al_2O_3), strontium sulfate ($SrSO_4$) and ferric oxide (Fe_2O_3) were used to obtain the appropriate mixtures calculated from the formula $3CaCO_3 \cdot (3-x)Al_2O_3 \cdot xFe_2O_3 \cdot SrSO_4$, where $x = 0$, 0.2, 0.4, 0.6, 0.8, 1.0, 1.2 and 1.4. The symbols and compositions of samples are shown in Table 1. Each sample was ground and mixed thoroughly; the appropriate amount of water was added to form a compact about 10 mm thick and 20 mm in diameter under pressure. After heating each sample in the form of a wet compact at a temperature of 1100–1350°C for 3 h, it was cooled in air and ground again to obtain the final product, which was stored in a desiccator.

The compressive strength of each sample was measured by using neat paste in a small mould ($2 \times 2 \times 2\ cm^3$) and a water/solid ratio (w/c) of 0.29. In order to investigate the possibility of producing a new kind of cement, calcium aluminate ($CaO \cdot Al_2O_3$) and calcium dialuminate ($CaO \cdot 2Al_2O_3$) were prepared by mixing $CaCO_3$ and Al_2O_3 thoroughly, grinding, moulding to form wet compacts which were sintered at 1400°C for 4 h, cooling in air and finally grinding to obtain the products. They were added to the $3CaO \cdot 3Al_2O_3 \cdot SrSO_4$. The two materials were mixed in the ratio 50 wt.%. These two samples were called SA and SA2, corresponding to the added $CaO \cdot Al_2O_3$ and $CaO \cdot 2Al_2O_3$ respectively.

TABLE 1

Compositions of the samples (wt.%)

Sample	$CaCO_3$	Al_2O_3	$SrSO_4$	Fe_2O_3
SF00	38.02	38.73	23.25	
SF02	37.47	35.62	22.92	3.99
SF04	36.94	32.61	22.60	7.85
SF06	36.42	29.68	22.28	11.62
SF08	35.92	26.83	21.97	15.28
SF10	35.43	24.06	21.67	18.84
SF12	34.95	21.36	21.38	22.31
SF18	34.49	18.74	21.10	25.68

The samples were mixed with water (w/c ratio 0.29), cured for one day in a humidity chamber and then cured in water at 25°C. At 3, 7 and 28 days the compressive strengths was measured.

SEM pictures were taken of some samples. The samples were immediately immersed in ethanol (AR grade) to obtain the SEM pictures. To obtain more information on the hydration products, residues were ground with ethanol to pass a 180-mesh sieve, washed once with ethanol and then twice with acetone, heated under vacuum at 50–60°C for 2–3 h, then heated at 60°C for 3 h. The products were stored in a desiccator.

All the surface area measurements were made by using the Blain permeability apparatus.

Apparatus

XRD

After mixing the sample with appropriate amounts of α-Al_2O_3 powder, a thin layer was exposed using the HZGA-PC X-ray diffractometer to obtain the exact positions of peaks. The Bragg equation was then used to calculate the lattice constants. The parameters of the X-ray diffractometer were $2\theta = 1/100$, the data collection interval was 2 s.

Microcalorimeter

By using the Setaram microcalorimeter HT-1500 the liberated heat of hydration at 30°C was measured on a sample with a w/c of 10.

DTA

DTA patterns were measured on the Shanghai DTA equipment with the following parameters. The sensitivity was equal to 10 mV and the heating rate was 10°C min^{-1}. The temperature range was from room temperature to 600°C.

SEM

The SEM pictures were obtained using the JEOL ISI-SX-40 electron microscopy equipment. The accelerating voltage was 20 kV.

RESULTS AND DISCUSSION

The maximum solid solution

As the amount or Fe_2O_3 in the SF system (see Table 1) compounds increased, the XRD peaks moved to a lower angle, which meant that the lattice constant increased. When the iron atoms in $3CaO \cdot 3Al_2O_3 \cdot SrSO_4$ reached a maximum, the lattice constant of $3CaO \cdot 3Al_2O_3 \cdot SrSO_4$ with iron atoms reached a constant value, which did not change even though

TABLE 2

Lattice constants a (Å) of the SF system

SF00	SF06	SF08	SF10	SF12	SF14
18.4852	18.5389	18.5458	18.5488	18.5489	18.5489

there were larger amounts of iron atoms in the mixture. The results of the lattice constant determinations are shown in Table 2 and Fig. 1; they indicate that in sample SF10 the amount of iron atoms in the compound has reached a maximum; in other words it is saturated with iron. However, from the results of XRD on the SF system compounds shown in Table 3, it is seen that not all of the Fe_2O_3 added stayed in the lattice of the compound: it can always also be found as C_xAF_{1-x} (mainly in C_2F form), with CA or C_3A also identified.

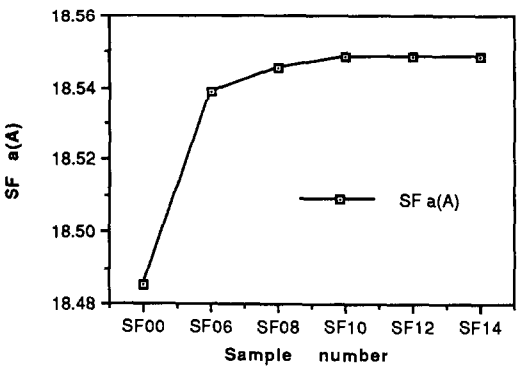

Fig. 1. The lattice constants of SG system compounds.

TABLE 3

XRD results of SF system compounds [a]

System	$3CaO \cdot 3Al_2O_3 \cdot SrSO_4$	C_xAF_{1-x} [b]	CA and C_3A
SF00	+ + + + + +	n	+
SF02	+ + + + + +	n	T
SF04	+ + + + + +	T	n
SF06	+ + + + +	T	n
SF08	+ + + + +	+	n
SF10	+ + + +	+	n
SF12	+ + + +	+ +	n
SF14	+ + + +	+ +	n

[a] T, trace amount; n, does not exist; the more +, the larger the relative amount of that component.

[b] Mainly in the form of C_2F.

Although we know the conditions at which the maximum solid solution amount of Fe_2O_3 in the compound is reached, the exact positioning of the iron atoms in the compound still poses a problem. There are two types of replacement in the crystal lattice. In the first type, the atoms of the lattice are directly replaced (Schottky defects). This kind of replacement makes the foreign atoms take part in the formation of the lattice. In the other type of defect, the minor atoms stay between the atoms of the lattice and do not take part in the formation of lattice (Frankel defects). The latter is also a kind of bulk effect. The results of XRD show that when the maximum solid solution condition is reached, there is always C_xAF_{1-x} (mainly in C_2F form) formed in the mixture, so we can say that there is always some Fe_2O_3 left behind, while some has reacted with the compound to form the first type of replacement, owing to the small difference between the radius of Fe^{3+} (0.57 Å) and Al^{3+} (0.47 Å). Therefore, the second type of replacement dominates.

Strength and the process of hydration

Strength of the compacts

Table 4 shows the compressive strengths of the SF system compounds and the SA and SA2 samples (see the section Experimental for the composition) and Figs 2 and 3 show the plots of strength vs. time of aging. From the data, the strengths of the compounds with Fe_2O_3 can be seen to be lower than that of the pure compound SFOO. This is due to the formation of unreactive C_xAF_{1-x} (mainly in C_2F form) in the sample. When calcium aluminate (CA) and calcium dialuminate (CA_2) are added to the pure compounds ($3CaO \cdot 3Al_2O_3 \cdot SrSO_4$), corresponding to SA and SA2 samples respectively, the early and later strengths are higher than those of the pure compound (sample SF00). The early strength of the SA sample still is slightly higher than that of SA2, which is due to the faster hydration rate of CA compound in the SA sample. When the long term strength is considered, the SA2 sample shows

TABLE 4

The compressive strengths of SF system compounds

Sample	Surface area ($cm^2 g^{-1}$)	Comp. strength ($kg cm^{-2}$)		
		3 Days	7 Days	28 Days
SF00	2756	426	667	841
SF04	2958	421	652	829
SF08	2990	405	642	801
SA	3021	507	726	915
SA2	3001	486	730	920

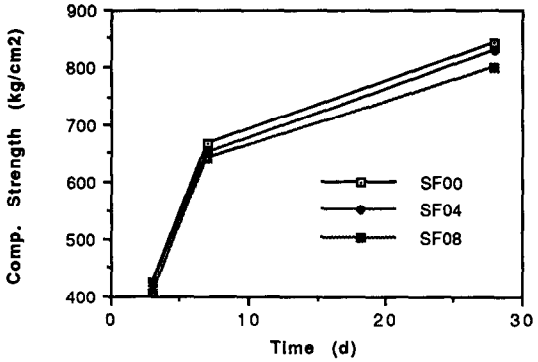

Fig. 2. Compressive strengths of SF00, SF04 and S08.

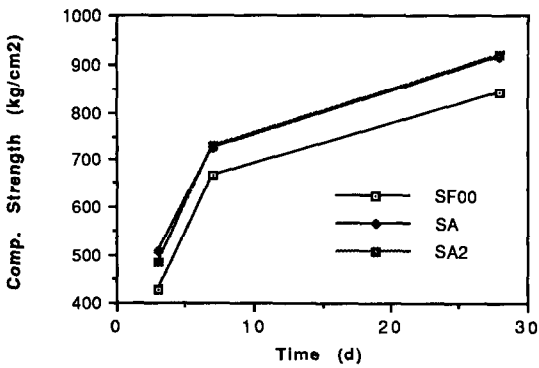

Fig. 3. Compressive strengths of SF00, SA and SA2.

to advantage, due to the low porosity, which is accounted for by the low initial hydration of CA_2. In order to give some explanation of the growth of strengths of samples, a study of their hydration is necessary.

The hydration process

Figures 4 and 5 show the hydration heat curves of SF00 and SF04 and patterns for the integration of hydration heat respectively. In Fig. 4, the obvious difference in the hydration curves shows that there is no induction period in the SF00 sample. Further, the hydration of SF00 is much faster than that of SF04, which takes about three times longer time to be completed. The presence of other oxide species in SF04 is the reason for the slowing down of the hydration process and causes the induction period.

The hydration products of various samples (at different curing times) determined by XRD are shown in Table 5. Figures 6, 7 and 8 show the DTA patterns of selected samples. From these results and previous research [2], the process of the hydration can be explained as follows.

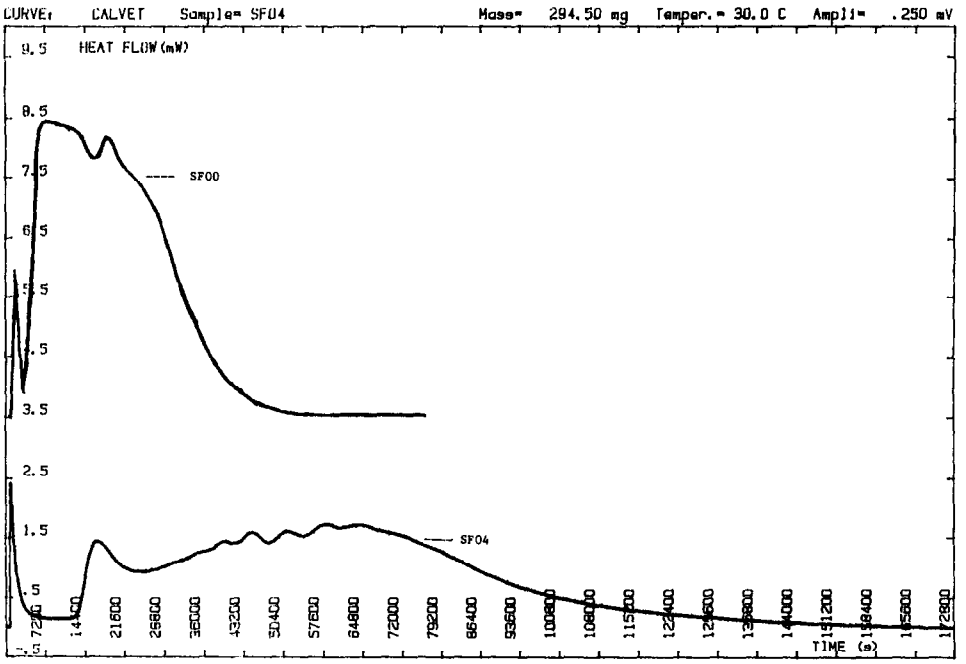

Fig. 4. The hydration curves of SF00 and SF04.

When water is added to the sample, the main component ($3CaO \cdot 3Al_2O_3 \cdot SrSO_4$) quickly hydrates and releases Ca^{2+}, Al^{3+}, Sr^{2+} and SO_4^{2-} ions. The ettringite-like hydrate is formed as the main hydration product with formula $3CaO \cdot Al_2O_3 \cdot 3SrSO_4 \cdot nH_2O$. At the same time, the aluminum gel ($Al(OH)_3$ or AH_3) is formed as the minor hydration product.

After the concentrations of ions in the liquid reach a certain level and enough hydration products cover the surface of the sample, the hydration

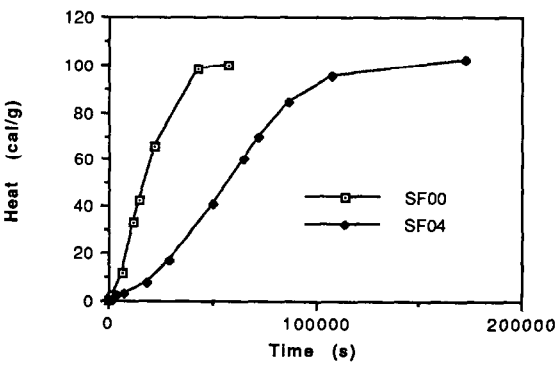

Fig. 5. The integrated hydration heats from the hydration heat curves.

TABLE 5

XRD results of the hydration products [a]

Sample	Days	Unreacted	SFt [b]	SFm [c]	C_4AH_{13}	C_2AH_8	AH_3
SF00	3	+ + + + +	+ +	–	T	–	+
	7	+ + + + +	+ +	–	+	–	+
	28	+ + + +	+	T	+ +	–	+
SF04	3	+ + + +	+ +	–	+	–	+ +
	7	+ + + +	+ +	–	+ +	–	+ +
	28	+ + +	+ + +	T	+ +	T	+ +
SF08	3	+ + + +	+ +	–	+	–	+ +
	7	+ + +	+ + +	T	+ +	T	+ +
	28	+ + +	+ + +	T	+ +	+	+ +
SA	3	+ + + +	+	–	T	–	+
	7	+ + + +	+	T	T	–	+ +
	28	+ + +	+ +	+	+	–	+ +
SA2	3	+ + + +	+	–	T	–	+
	7	+ + + +	+	T	T	–	+ +
	28	+ + +	+ +	T	+	–	+ +

[a] T, trace amount; the more +, the larger the relative amount of that component. [b] This is the symbol for the hydrate which has similar XRD and DTA patterns to those of ettringite. [c] This is the symbol for the hydrate which has similar XRD and DTA patterns to those of monosulfate calcium aluminate hydrate.

process arrives at an induction or dormant period. In this dormant stage the diffusion process is very slow because of the covering of the sample's surface by the hydration products and the common ion effect while the concentrations of ions are increasing. It is shown as the flat period in the hydration heat curves of the SF04 sample. However, in the SF00 sample there is a very short induction period and this is due to the crystals formed in the initial hydration step being too few to cover the surface of the reactant. Further, the other oxide species cause the rapid increase in the concentrations of the ions in the liquid.

When the concentrations of ions in the liquid reach a certain level, calcium aluminate hydrate and other hydrates crystalize again. The sudden reduction in the concentration of ions in the liquid phase and in the size of the contracting unreacted particles is due to hydration making the diffusion process faster. The hydration process then proceeds at an accelerating rate. As the hydration progresses, the rate of the hydrolysis becomes faster than that of the crystal growth, which makes the concentrations of ions in the liquid phase reach another saturated level and causes the hydration process to slow down. This explanation is the reason for the appearance of the small hill-like period in the accelerating part of the hydration heat curves. At this time the unreacted samples become very small fragments and can react with water very easily. The

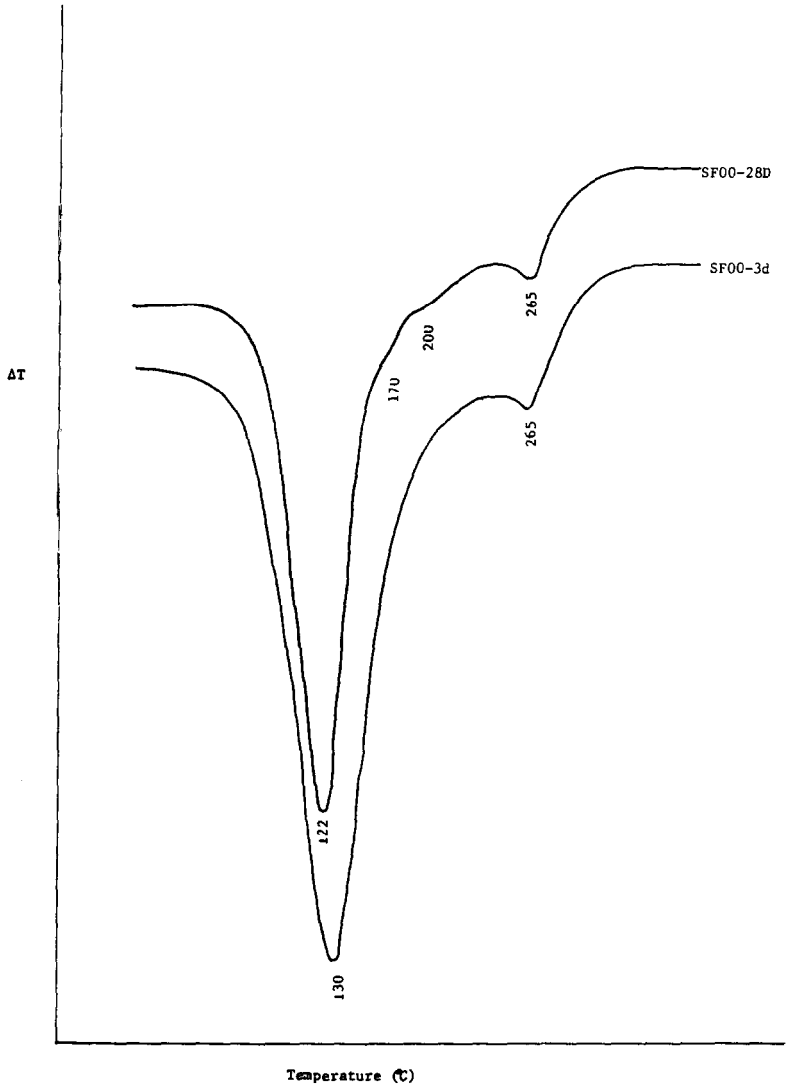

Fig. 6. The DTA curves of hydrated SF00 samples at 3 days and 28 days.

hydration of these fragments is the final stage in the hydration process. This causes the final peaks in the hydration heat curves.

While Fe_2O_3 is present in the sample, the initial hydrated products have greater porosity and thus cause the lower initial strengths. However, for the final strength, the process of hydration causes the pores to be filled and has little effect on their final strengths. The SEM results in Fig. 9 show the difference of porosity and interaction among particles.

The DTA data analysis

According to previous research on the DTA patterns of cement

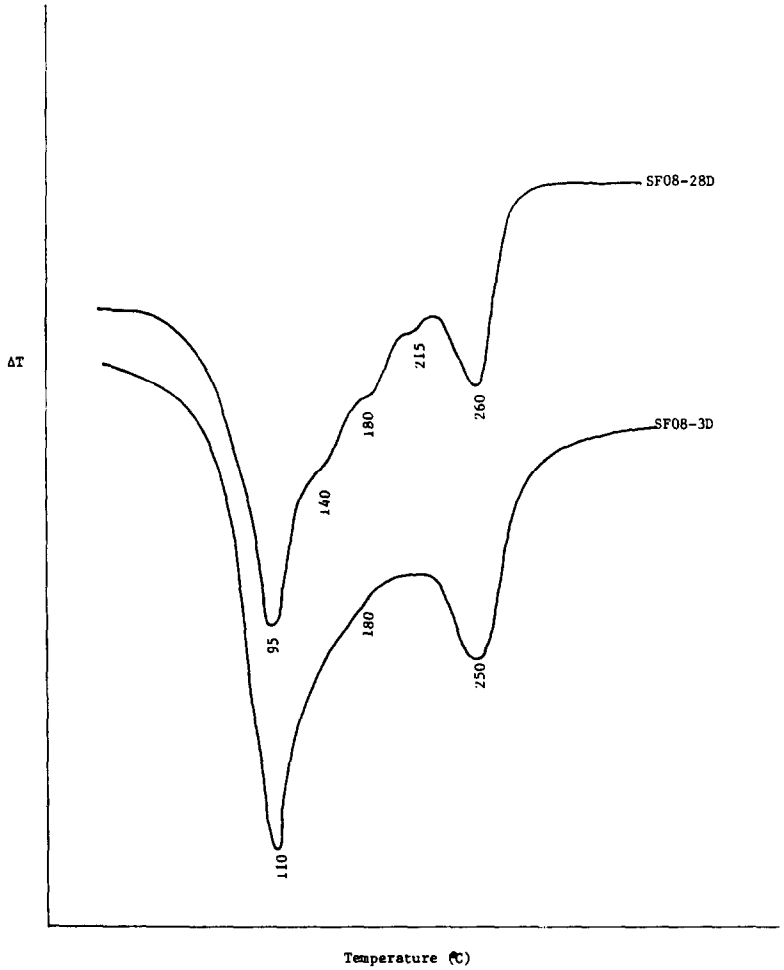

Fig. 7. The DTA curves of hydrated SF08 samples at 3 days and 28 days.

hydration products [3, 4], peaks around 120°C correspond to the dehydration of ettringite or CAH_{10}, peaks around 140°C correspond to the dehydration of C_2AH_8, peaks around 200°C correspond to the dehydration of C_4AH_{13}, peaks around 260°C correspond to the dehydration of AH_3, and peaks around 180°C correspond to the dehydration of the monosulfate calcium aluminate hydrate (AFm).

From the DTA patterns of SF00, SF04 and SA samples of various ages, it is found that there are peaks around 120°C which may be due to the dehydration of the CAH_{10} or the hydrate which has a similar form to ettringite ($3CaO \cdot Al_2O_3 \cdot 3CaSO_4 \cdot 32H_2O$). From the XRD results (Table 5), there was no CAH_{10} formed in the samples whereas there were XRD peaks very similar to those of ettringite. This means that a new hydrate similar to ettringite was formed in these samples. The formula for this

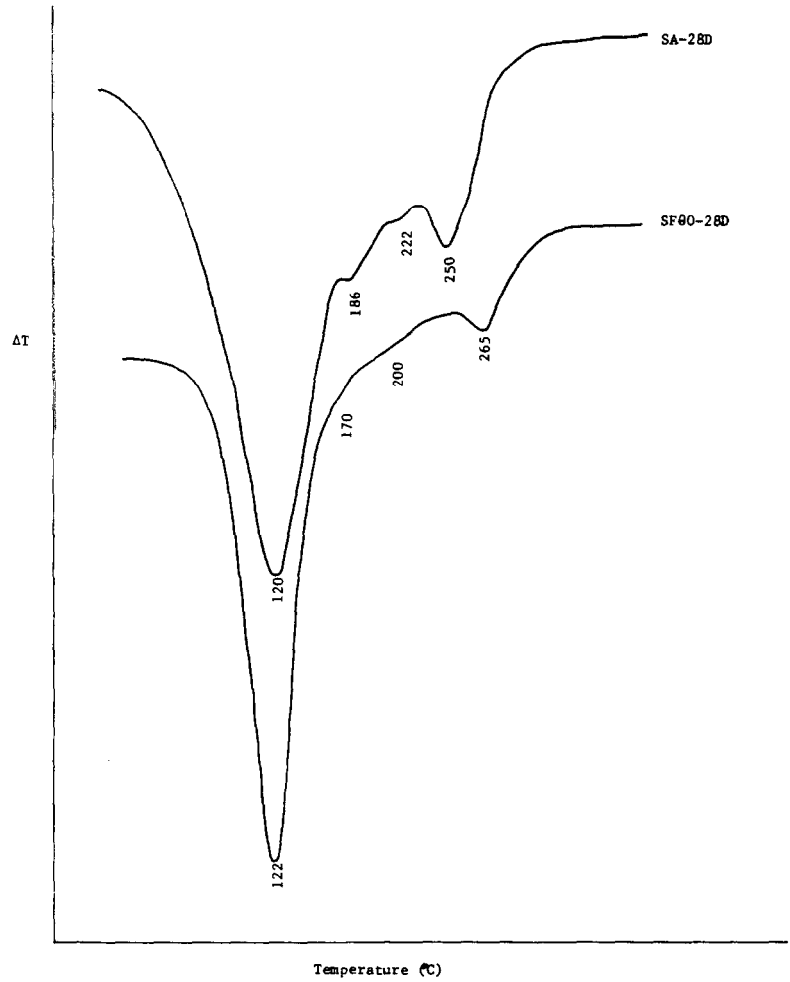

Fig. 8. The DTA curves of hydrated SF00 and SA samples at 28 days.

hydrate is proposed as $3CaO \cdot Al_2O_3 \cdot 3SrSO_4 \cdot nH_2O$. Examination of both the DTA and XRD patterns after a very long hydration time, especially for the SF08 sample at 28 days, show a peak around 180°C which would correspond to the dehydration of AFm. This leads to the postulation of another hydrate $3CaO \cdot Al_2O_3 \cdot SrSO_4 \cdot nH_2O$.

The hydration processes of these samples can then be postulated as the formation of ettringite-like hydrates $3CaO \cdot Al_2O_3 \cdot 3SrSO_4 \cdot nH_2O$ and AH_3 in the initial stage, followed by the formation of the monosulfate hydrate, $3CaO \cdot Al_2O_3 \cdot SrSO_4 \cdot nH_2O$, C_2AH_8, and C_4AH_{13}, where C_2AH_8 is only formed in the samples with Fe_2O_3.

From the peak temperatures and the XRD results, there was no C_3AH_6 formed in any of the samples, especially not in the SA and SA2 samples in

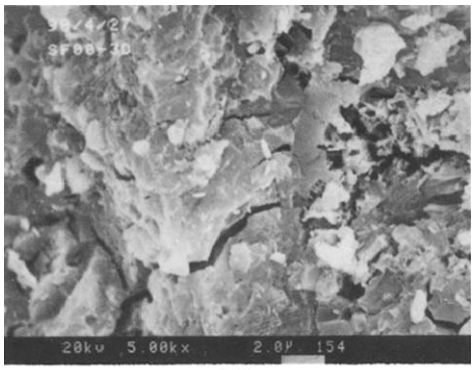

(a)

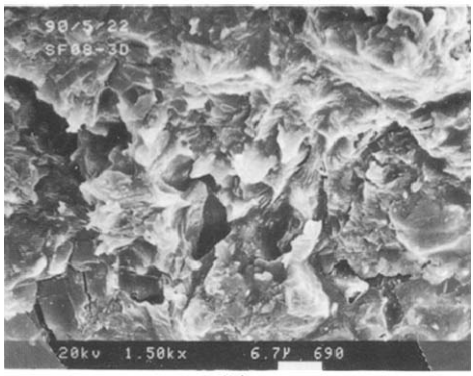

(b)

Fig. 9. Scanning electron micrographs. Original magnifications at 5000× and 1500×: (a), hydrated SF00 sample at 3 days (original magnification 5000×); (b), hydrated SF08 sample at 3 days (original magnification 1500×). Note that the porosity in (b) is much larger than that in (a), which accounts for the low compressive strength of the (b) sample.

which CA and CA_2 were introduced. This property can prevent the intrinsic danger of the fracture of concrete due to the expansion caused by the transformation of calcium aluminate hydrates into cubic C_3AH_6.

CONCLUSIONS

(1) The condition for Fe_2O_3 to reach the maximum solid solution in $3CaO \cdot 3Al_2O_3 \cdot SrSO_4$ is about 18.84 wt.% Fe_2O_3 in the preparation process.

(2) The addition of Fe_2O_3 causes a slight decrease in the compressive strength, which is due to the formation of C_xAF_{1-x} (mainly in C_2F form).

(3) Upon hydration there are two hydrates found. They are similar to ettringite and the monosulfate hydrate; the proposed formulae are $3CaO \cdot Al_2O_3 \cdot 3SrSO_4 \cdot nH_2O$ and $3CaO \cdot Al_2O_3 \cdot SrSO_4 \cdot nH_2O$ for the trisulfate and monosulfate forms respectively.

(4) The hydration processes of $3CaO \cdot 3Al_2O_3 \cdot SrSO_4$ are

$$3CaO \cdot 3Al_2O_3 \cdot SrSO_4 + H_2O \rightarrow 3CaO \cdot Al_2O_3 \cdot 3SrSO_4 \cdot nH_2O + AH_3 + \text{calcium aluminates hydrates (minor)}$$

$$3CaO \cdot Al_2O_3 \cdot 3SrSO_4 \cdot nH_2O \rightarrow 3CaO \cdot Al_2O_3 \cdot SrSO_4 \cdot nH_2O + \text{calcium aluminate hydrate (minor)}$$

(5) There is no C_3AH_6 formed (which would have caused a reduction in strength), even when CA and CA_2 are added to the sample. This property makes the manufacture of high early- and final-strength aluminum sulfate cements possible.

ACKNOWLEDGMENTS

D.C. acknowledges that all the work was performed under the guidance of Prof. Dr.-Ing. Feng. We are also very appreciative of our colleagues, Dr. Hu Shuguang, Mr. Liao, etc., who helped us with the difficult experiments.

REFERENCES

1 I. Teoreanu, M. Muntean and I. Dragnea, Cemento, 83(1) (1986) 39.
2 L. Guangling, Thesis for Master's degree, The Wuhan University of Technology, 1986.
3 V.S. Ramachandran, Application of DTA in Cement Chemistry, Chemical Publishing Co., New York, 1969.
4 M. Murat, Proc. Int. Sem. on Calcium Aluminates, Turin, 1982, Polytechnico di Torino, 1982, p. 59.